sustainability

MDPI

Article

Large-Scale Flood Hazard Monitoring and Impact Assessment on Landscape: Representative Case Study in India

Bijay Halder [1], Subhadip Barman [2], Papiya Banik [3], Puja Das [4], Jatisankar Bandyopadhyay [1], Fredolin Tangang [5], Shamsuddin Shahid [6], Chaitanya B. Pande [7,8,9], Baqer Al-Ramadan [10] and Zaher Mundher Yaseen [11,12,*]

1 Department of Remote Sensing and GIS, Vidyasagar University, Midnapore 721102, India
2 Centre for Environmental Studies, Vidyasagar University, Midnapore 721102, India
3 Department of Geography, University of Calcutta, Kolkata 700019, India
4 Department of Geography, Cotton University, Guwahati 781001, India
5 Department of Earth Sciences and Environment, Faculty of Science and Technology, Universiti Kebangsaan Malaysia, Bangi 43600, Selangor, Malaysia
6 Department of Water and Environmental Engineering, Faculty of Civil Engineering, Universiti Teknologi Malaysia (UTM), Skudia 81310, Johor, Malaysia
7 Indian Institute of Tropical Meteorology, Pune 411008, India
8 Institute of Energy Infrastructure, Universiti Tenaga Nasional, Kajang 43000, Selangor, Malaysia
9 New Era and Development in Civil Engineering Research Group, Scientific Research Center, Al-Ayen University, Thi-Qar, Nasiriyah 64001, Iraq
10 Architecture and City Design, King Fahd University of Petroleum & Minerals, Dhahran 31261, Saudi Arabia
11 Civil and Environmental Engineering Department, King Fahd University of Petroleum & Minerals, Dhahran 31261, Saudi Arabia
12 Interdisciplinary Research Center for Membranes and Water Security, King Fahd University of Petroleum & Minerals, Dhahran 31261, Saudi Arabia
* Correspondence: z.yaseen@kfupm.edu.sa

check for updates

Citation: Halder, B.; Barman, S.; Banik, P.; Das, P.; Bandyopadhyay, J.; Tangang, F.; Shahid, S.; Pande, C.B.; Al-Ramadan, B.; Yaseen, Z.M. Large-Scale Flood Hazard Monitoring and Impact Assessment on Landscape: Representative Case Study in India. *Sustainability* **2023**, *15*, 11413. https://doi.org/10.3390/su151411413

Academic Editor: Mike Spiliotis

Received: 23 May 2023
Revised: 19 July 2023
Accepted: 20 July 2023
Published: 23 July 2023

Abstract: Currently, natural hazards are a significant concern as they contribute to increased vulnerability, environmental degradation, and loss of life, among other consequences. Climate change and human activities are key factors that contribute to various natural hazards such as floods, landslides, droughts, and deforestation. Assam state in India experiences annual floods that significantly impact the local environment. In 2022, the flooding affected approximately 1.9 million people and 2930 villages, resulting in the loss of 54 lives. This study utilized the Google Earth Engine (GEE) cloud-computing platform to investigate the extent of flood inundation and deforestation, analyzing pre-flood and post-flood C band Sentinel-1 GRD datasets. Identifying pre- and post-flood areas was conducted using Landsat 8–9 OLI/TIRS datasets and the modified and normalized difference water index (MNDWI). The districts of Cachar, Kokrajhar, Jorhat, Kamrup, and Dhubri were the most affected by floods and deforestation. The 2022 Assam flood encompassed approximately 24,507.27 km^2 of vegetation loss and 33,902.49 km^2 of flood inundation out of a total area of 78,438 km^2. The most affected areas were the riverine regions, the capital city Dispur, Guwahati, southern parts of Assam, and certain eastern regions. Flood hazards exacerbate environmental degradation and deforestation, making satellite-based information crucial for hazard and disaster management solutions. The findings of this research can contribute to raising awareness, planning, and implementing future disaster management strategies to protect both the environment and human life.

Keywords: Assam flood inundation; vegetation degradation; risk assessment; Google Earth Engine; Sentinel-1 SAR data

1. Introduction

Floods are significant natural disasters that often result in extensive property damage and human suffering worldwide [1–4]. These high-magnitude events can cause massive geomorphic changes and significant alterations to the terrain [5–7]. India is one of the most disaster-prone countries globally, experiencing numerous environmental calamities every year [8–11]. Among these, floods are India's most frequent and devastating natural disasters. According to researchers and the UN's sustainable development goals, floods were the deadliest natural hazard between 1995 and 2015, affecting an estimated 2.3 billion people and resulting in 157,000 recorded fatalities worldwide [12,13]. The Brahmaputra River has an average depth of 100 ft (30 m) and can reach a maximum depth of around 440 ft (135 m). Its annual average discharge is approximately 700,000 cubic feet per second (19,000 m^3/s), while floodwaters can reach up to 3,500,000 cubic feet per second (100,000 m^3/s) [14]. The Ganga–Brahmaputra river delta exhibits the world's third-highest average discharge, around 1,086,500 cubic feet per second (30,770 m^3/s). It also carries the highest amount of suspended sediment, with an annual load of approximately 1.87 billion tonnes [14]. Flood inundation predominantly affects the Mymensingh and Jamalpur districts in the lower Brahmaputra River region.

Indian floods occur during the southwest monsoon season, which starts in June and extends until October. The incessant rainfall during this period leads to the overflowing of major Himalayan rivers [15]. Over the past two decades (2002–2022), floods have damaged 40 million hectares of land, causing losses of approximately USD 608 million and displacing nearly 10% of the Indian population. The states most prone to floods are Uttar Pradesh, Assam, Bihar, and West Bengal [16]. The Ganga and Brahmaputra river basins are particularly vulnerable to flooding, with the Brahmaputra River basin presenting a severe risk [17–19]. The northeastern region of India frequently experiences natural disasters such as floods, earthquakes, cyclones, landslides, and occasional droughts [20,21]. In Assam, flooding results in significant property damage and abruptly disrupts society. Every year during the monsoon season, the Brahmaputra River and its tributaries cause devastating floods, causing widespread destruction. Floods are widespread in the lower parts of the Brahmaputra River Basin, which covers 12.25% of the total topographical area and is prone to flooding in Assam [22]. Some major tributaries of the Brahmaputra River have extensive basin areas, with the Subansiri River alone covering 32,640 km^2, accounting for 7.92% of the total Brahmaputra River Basin area. Refer to Table 1 for detailed information on various tributaries of the Brahmaputra River.

Table 1. Details about the tributaries.

River Name	Total Area (Km^2)	Discharge (cu ft./s)	
		Maximum	Minimum
Subansiri River	32,640	663,900	4600
Barak River	52,000	562,400	4934
Kolong River	250	5218.75	1450
Dhansiri River	1220	3520	1204
Manas River	41,350	7641	6521

Flooding in Assam state is primarily caused by heavy rainfall and specific geo-climatic conditions during the monsoon season. The most severe recorded flood since 1998 occurred in 2012, affecting 21 out of 27 districts. Even during the COVID-19 pandemic, Assam experienced floods that impacted 2 to 3 million residents in 27 districts [23]. In June 2022, the meteorological department of Assam reported rainfall of nearly 652.6 mm, surpassing the normal rainfall of 404.1 mm. The neighboring state of Meghalaya also received significant rainfall, with 1457.9 mm compared to the normal 697.3 mm. Flooding annually destroys natural vegetation, including wildlife, prompting animals in wildlife sanctuaries to seek higher ground for safety [24]. In 2022 flood inundations severely affected portions of the Pobitora Wildlife Sanctuary and Kaziranga National Park, leading animals to move to higher areas for protection [9,25].

Vegetation is crucial in preventing soil erosion, mitigating environmental degradation, reducing landslide occurrences, and minimizing flood hazards [26–28]. During the 2022 Assam flood, it was essential to identify damaged green spaces, as it provides valuable insights for ecological diversity analysis beyond studying inundated areas. Sentinel-1 C band SAR datasets and the GEE platform were extensively used, specifically examining deforested land and calculating the inundation area using threshold values in GEE. The Sentinel-1 C band datasets were instrumental in high-resolution flood hazard mapping [25,29,30]. The main objectives of this study are to evaluate the impact of the 2022 Assam flood on land use, land cover, inundation areas, and deforested lands. This was achieved using Sentinel-1 C band GRD SAR data and the GEE cloud computing platform. The analysis focuses on accurately measuring the extent of inundation and identifying areas with vegetation damage using high-resolution microwave SAR datasets. Such information is crucial for monitoring vegetation health and flood hazards during flood events. The recent Assam flood has caused significant devastation, underscoring the need to identify areas prone to hazards and assess vegetation damage for effective disaster management and awareness campaigns. This study's outcomes, which concentrate on the 2022 Assam Flood, provide novel insights, making them particularly valuable for decision-making, raising awareness, and implementing mitigation measures. Additionally, identifying locations with vegetation damage can facilitate the development of innovative adaptation strategies to protect forested lands, which is vital for environmental conservation. The findings of this investigation can support local planners, administrators, researchers, and management departments in Assam state, aiding in saving lives and assisting in post-disaster planning.

2. Study Area

Assam, located in northeastern India, is the most populous and second-largest state. It holds significant importance in India from geographical, demographic, cultural, and environmental perspectives, as it is home to various cultural aspects. Geographically, Assam spans from 22°19′ N to 28°16′ N latitude and 89°42′ E to 96°30′ E longitude, covering an area of 78,438 km^2. The state shares borders with West Bengal to the west; Meghalaya, Tripura, Mizoram, and Bangladesh to the south; Bhutan and Arunachal Pradesh to the north; and Nagaland, Arunachal Pradesh, and Manipur to the east (Figure 1). The Ganga–Brahmaputra–Meghna river delta, known for its fertile land and vegetation, plays a crucial role in the region. However, this delta is prone to various natural disasters. Assam, located within the Brahmaputra River basin, experiences the influence of numerous tributaries, which can cause damage to vegetation [18,31] and crop production through suspended sediment and river discharge. Floods in the region are attributed to climate change, vegetation degradation, and significant riverbank erosion. It is not only Assam but also other areas along the Brahmaputra River that are affected by high river discharge. The state is divided into 33 administrative districts. Assam's climate is predominantly tropical monsoon, characterized by high humidity and heavy rainfall. As of the 2011 Census, Assam accounted for 2.58% (31,205,576 people) of the total Indian population, with a population density of 398 km^2 (Figure 2). The state's overall literacy rate is 72.19%, with 77.85% for males and 66.27% for females. The research area exhibits a rich diversity of ethnic cultures, including Boro, Deori, Rava, Karbi, Assamese, Bengali, Ahom, and Rajbanshi, among others, as well as a wide variety of flora and fauna, rivers, and natural resources. Some significant rivers in Assam include the Brahmaputra, Subansiri, Bhogdoi, Barak, Kolong, Dhansiri, and Manas.

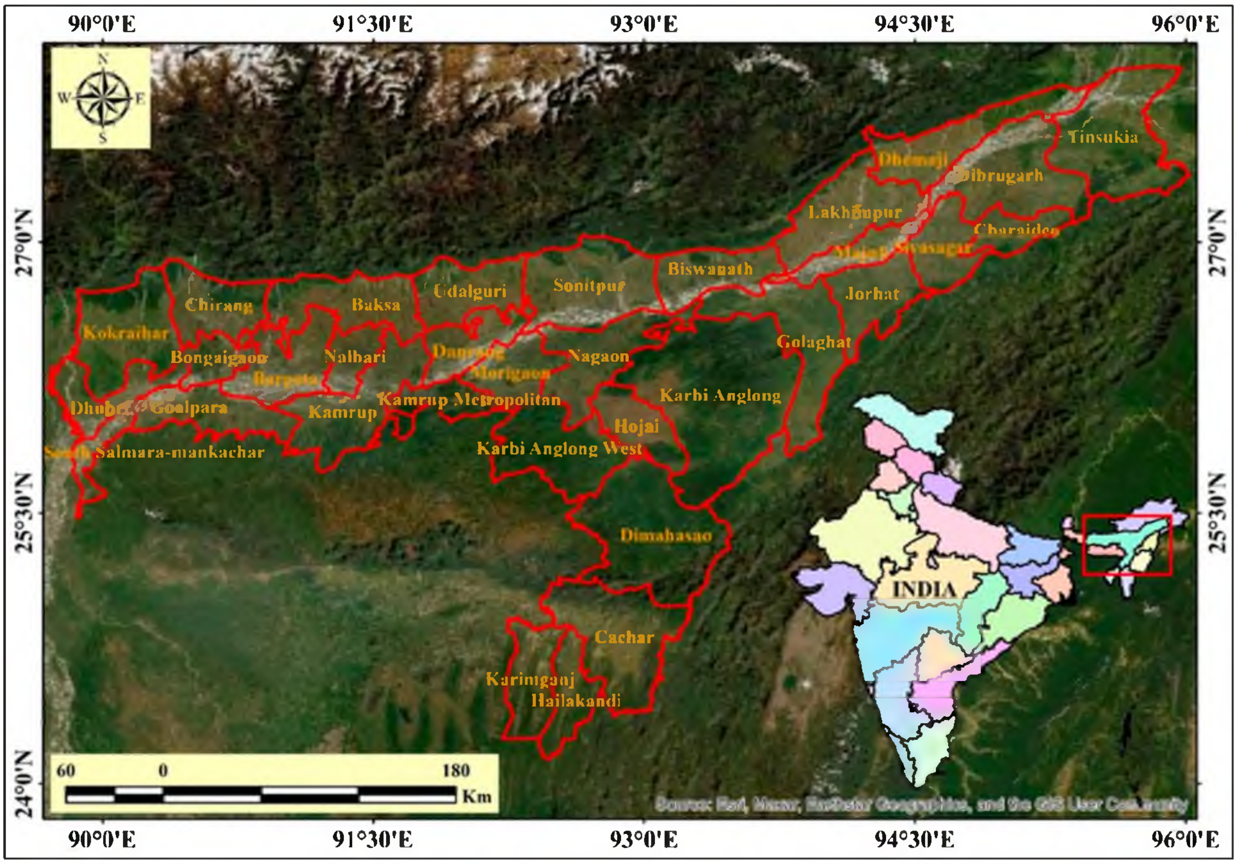

Figure 1. Locational map of the study area.

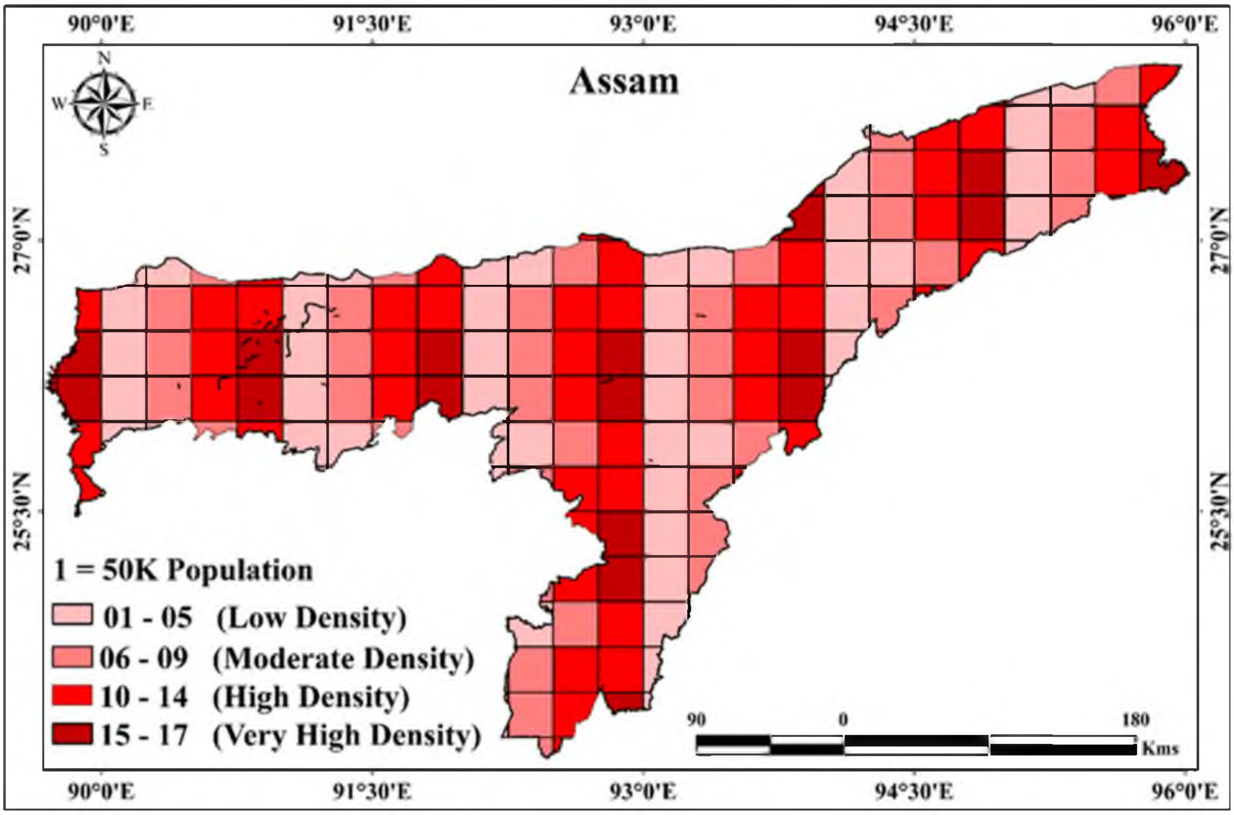

Figure 2. Grid-wise population density map of Assam (Source: Census of India, 2011).

2.1. Causes of the Floods in Assam

Assam state faces severe flood damage every year due to the heavy rainfall experienced during the monsoon season [25,32]. The Brahmaputra valley receives an average annual rainfall of around 2480 mm while the northeastern hills receive 6350 mm. The Water Resource Department of Assam attributes the floods in the state to the abundant and sometimes extreme rainfall during the monsoon season. In June 2022, the state recorded 652.6 mm of actual rainfall, surpassing the normal 404.1 mm. Drainage congestion is another factor contributing to floods, where high water levels in the Brahmaputra River impede the discharge of tributaries, leading to backflow and congestion near outfalls. Insufficient drainage through sluices and encroachment on natural drainage systems exacerbate the situation. Limited waterways in culverts and bridges on railroads and roads hinder the natural water flow.

Flood inundation is also caused by encroachment on riverine areas, as the narrowness of the valley and limited available plain land for settlements contribute to the problem. The high population density of over 200 inhabitants per km^2 in the plains directly affects drainage patterns. The increase in population and development activities has led to encroachment on “chars” (riverine islands). The region’s frequent tectonic activity, including earthquakes and landslides, contributes to flood inundation in Assam. The Brahmaputra Valley, located in Zone V with a high danger level, experiences frequent changes in the river’s course due to the excessive sediment load. This results in the river overflowing its banks or eroding, as its capacity to carry sediment is limited. Deforestation also plays a role in flooding. Ongoing deforestation in Assam leads to topsoil erosion during heavy rainfall, causing significant amounts of sediment to be carried downstream into rivers. This accumulation of silt and sediment raises the river levels.

2.2. Flood History of Assam

Assam state is prone to frequent flooding and faces significant flood risks. While floods have always been common in riverine areas, the severity of the damage caused by floods has increased in recent years. The Brahmaputra valley, with more than 40% of its land vulnerable to flood damage, has an area of approximately 3.2 million hectares affected by floods [33]. Assam has experienced devastating floods in several years, including 1954, 1966, 1972, 1975, 1978, 1983, 1986, 1996, 1998, 2000, 2002, 2012, 2014, and 2020.

According to records from the Assam State Disaster Management Authority (ASDMA), some of the most destructive floods in recent years occurred in 2012, affecting 21 out of the state’s 27 districts. In 2013, heavy rainfall caused floods that devastated around 7000 hectares of agricultural land in 12 districts, affecting 396 villages. The year 2014 damaged 1846 settlements and displaced nearly 1.6 million people. In 2015, there were 1031 affected villages, and around 1.5 million people were displaced. In 2016, almost one million people in Assam were devastated by floods, with Morigaon, Barpeta, and Goalpara being the most severely affected districts out of the 21. Floodwaters affected nearly 3000 settlements in 21 districts, impacting over 100,000 people. In 2022 flooding in Lakhimpur, Karimganj, and Kokrajhar districts has forced the relocation of over 1.7 million people and has affected approximately 2450 villages [34].

In 2018, floods in the tributaries of the Brahmaputra affected 450,000 individuals in eight districts of Assam. The initial wave of floods that year claimed the lives of 12 people [ASDMA report]. In 2019, 30 districts and 5,259,142 people were severely affected, along with 163,962.02 hectares of cropland. By July 20, 59 people had died, and 22 districts with 3024 villages were affected. The 2020 Assam flood coincided with the COVID-19 pandemic and had a significant impact. The initial floods in May 2020 affected nearly 30,000 people and destroyed crops in five districts. As of October 2020, 123 people had died from floods, while 26 people lost their lives due to landslides. The floods affected nearly five million people, with over 150,000 seeking refuge in shelters and 5474 villages being affected [35].

3. Materials and Method

3.1. Data and Software Used

Multi-date Sentinel-1 SAR C band GRD images were utilized to calculate vegetation degradation and inundation during the recent Assam flood in May 2022. The Sentinel-1 SAR datasets were employed to estimate the extent of flood inundation and vegetation damage across different regions of Assam. This analysis was conducted using the cloud-computing-based Google Earth Engine (GEE) platform to generate inundation maps and assess vegetation damage [28,29]. The ESRI Sentinel-2 multispectral images with a 10 m resolution were employed for evaluating the impact on the landscape. Pre-flood and post-flood data from Sentinel-1A/B Ground Range Detected (GRD) were used to determine the areas affected by flood inundation and vegetation damage during the Assam 2022 flood. The Vertical Horizontal (VH) and Vertical Vertical (VV) datasets from Sentinel-1 SAR were utilized. The pre-flood data covered the period from 1 March 2022 to 30 April 2022, while the during/post-flood data spanned from 26 May 2022 to 20 June 2022. Landsat 8 OLI/TIRS datasets were employed to identify space-based water fluctuation using the modified normalized difference water index (MNDWI). The Landsat datasets were obtained from the USGS Earth Explorer website (https://earthexplorer.usgs.gov/, accessed on 20 August 2022). The pre-flood and post-flood Landsat data corresponded to 4 March 2022, and 24 June 2022, respectively. The land use and land cover data were derived from the freely available ESRI Sentinel-2 images with a 10 m resolution (https://www.arcgis.com/apps/instant/media/index.html?appid=fc92d38533d440078f17678ebc20e8e2, accessed on 22 August 2022).

3.2. Image Classification

After processing the raw data, the most common image processing method involves organizing and constructing pixels based on their digital numbers (DN). The images were then classified using supervised classification techniques in the GEE platform, using the spectral signatures of different land cover features. These features could be identified through a remote sensing-based (RS-based) dataset [36]. Land use and land cover (LULC) classification resulted in the desired number of classes [37]. These classes were then used to calculate the area covered by each class, facilitating the measurement of changes or differences in the area over the observation period. The classification accuracy was assessed in the next step. In our study, six LULC classes were defined for Assam state, including built-up areas, water bodies, trees, bare land, flooded vegetation, and croplands. The supervised image classification method, specifically the Maximum Likelihood technique, was implemented to categorize the identified features using the GEE platform.

3.3. SAR Data Pre-Processing and the GEE Platform

The GEE platform was utilized to delineate the extent of inundation and vegetation degradation caused by the 2022 flood in Assam. The flood significantly impacted the lower parts of the Brahmaputra River basin and the northern parts of West Bengal state and Bangladesh, particularly the north and northeastern regions. The GEE platform, which operates on cloud computing, combined with Sentinel-1 data (pre-flood and post-flood), was employed for this analysis. The Interferometric Wide (IW) swath approach datasets with a pixel spacing of 10 m and a swath width of 250 km were used [29,38]. The incident angle of the data ranged from 30° to 45°. The Sentinel-1 datasets provided information on the flood extent, forest cover, agricultural areas, and land deformation, and these datasets were obtained from the Copernicus Open Access Hub (https://scihub.copernicus.eu/, accessed on 20 August 2022). The atmospheric correction is necessary to generalize the SAR images, which helps reduce SAR data filtering [39,40]. The SAR data underwent pre-processing steps, including the application of orbit files, thermal noise removal, radiometric calibration, removing GRD image noise, atmospheric correction, and terrain Doppler correction [8,41].

Calibration approaches are widely employed to correct SAR observational activities. For radiometric calibration, it is recommended to use GPS-based ground network analysis, as well as Medium Resolution Imaging Spectrometer (MERIS) and Moderate Resolution Imaging Spectroradiometer (MODIS) data. The GEE cloud computing platform is extensively utilized for analyzing changes in the Earth's surface using various satellite data sources [42,43]. This platform offers the advantage of monitoring large-scale data but may require more time for software-based estimation. In the case of the 2022 Assam flood, the Level-1 C band GRD datasets were utilized to delineate the flooded area and vegetation degradation. The GEE platform was also employed to identify and select the relevant datasets, filter the pre- and post-flood data, perform histogram equalization, and conduct important statistical analyses to identify the flooded area. The resulting flood inundation and vegetation degradation data were exported to Google Drive in GeoTIFF format, with a CSV file used for histogram generalization.

3.4. MNDWI Estimation

Landsat 8 OLI/TIRS data was utilized to monitor the flooded areas. However, due to cloud cover, multispectral datasets were unavailable. Fortunately, certain parts of the study area were free from clouds, allowing them to identify the pre and post-flood inundation areas. The modified version of NDWI (Normalized Difference Water Index) was extensively employed for delineating the water areas. Equation (1) was used for conducting the MNDWI investigation [44,45].

$$\mathrm{MNDWI} = \frac{(\mathrm{Green} - \mathrm{SWIR1})}{(\mathrm{Green} = \mathrm{SWIR1})} \tag{1}$$

The 'raster calculator' of ArcGIS version 10.8 was used to calculate the flood inundation area.

3.5. Flood Inundation and Vegetation Degradation Estimation

This study used the Random Forest (RF) classifier, which uses many trees to analyze the classification problem. RGB Co-registration was utilized for pre-flood and post-flood threshold identification, while Grey Level Co-occurrence Matrix (GLCM) analysis was conducted on Sentinel-1 SAR datasets using 350 random samples. A total of 70% of the data points (245 points) were used for training, and the remaining 30% (105 points) were used for testing. GeoTIFF data exports were processed in the ArcGIS v10.8 platform, employing pixel-based area calculations and an overlapping approach to analyze land use and land cover (LULC) classes. GRD Sentinel-1 Level 1 SAR datasets were also utilized to assess vegetation degradation in Assam state, India. The study used the latest cloud computing platform, which facilitated delineating vegetation losses, LULC classification, identification of geospatial indices, air quality monitoring, and various planetary studies. The RF and the Classification and Regression Trees (CART) algorithms were employed within the Google Earth Engine (GEE) platform to identify areas of vegetation loss. Multiple sets of observational datasets, including training and testing, were used for this purpose.

3.6. Affected LULC Area Investigation

The LULC classification in this study utilized large-scale Sentinel-2 10 m datasets. The classification map was obtained from the freely available ESRI website. Three titles were obtained from the site and subsequently merged and clipped to create a comprehensive classification map. The district-wise calculation of LULC-affected lands was performed using overlapping and union/intersect techniques. The provided ESRI LULC classification map exhibited an accuracy of 85%, with predominant LULC features including trees, built-up land, rivers, flooded vegetation, and bare land. The affected lands were calculated district-wise by overlapping the LULC classes with flooded areas. The flood primarily impacted vegetation, built-up land, and croplands.

4. Results

Flash floods in neighboring areas such as Meghalaya and Arunachal Pradesh flowed through rivers passing Assam, worsening the state's flood situation. In June 2022, the region experienced extremely intense flash floods due to cloudbursts in the catchment areas of Meghalaya and Arunachal Pradesh. These flash floods resulted in numerous fatalities and widespread devastation across a large area. At the New Haflong railway station in the Dima Hasao district, train coaches were overturned by mudslides triggered by heavy rainfall. The Assam floods, devastating natural phenomena in the humid tropics, highlight the interplay between the monsoon season and flood inundation. Understanding this relationship is crucial for hazard risk assessment, planning, and decision-making by disaster management authorities, as well as for implementing measures to reduce future disasters, raise awareness, develop adaptation strategies, and formulate policies [46,47].

4.1. Flood Inundation and Deforested Land Identification

The 2022 Assam flood had a devastating impact, resulting in significant losses. This study aimed to identify the flood inundation lands and deforested areas in Assam state caused by the 2022 flood. Figure 3 illustrates the analysis of space-based water areas using pre- and post-satellite datasets to identify water bodies. The Modified Normalized Difference Water Index (MNDWI) was used to delineate water areas, with the post-MNDWI map highlighting high water areas. The investigation focused on the capital city Dispur to identify MNDWI-based water locations. Figure 4a presents the overall flood-inundated land of Assam, and district-level inundated areas are listed in Table 2. Additionally, Figure 4b displays the overlap of flood-inundated lands on the Normalized Difference Vegetation Index (NDVI) map, calculated using the Google Earth Engine (GEE) platform. Various parts of the state were affected, such as Kokrajhar (2213.64 km^2), Tinsukia (847.94 km^2), Dhemaji (1445.28 km^2), Dibrugarh (698.78 km^2), Lakhimpur (842.97 km^2), Jorhat (942.91 km^2), Dimahasao (1759.34 km^2), Cachar (2253.29 km^2), Karimganj (1095.16 km2), Karbi Anglong West (1795.28 km^2), Nagaon (1594.72 km^2), Morigaon (1056.38 km^2), Sonitpur (1549.24 km^2), Kamrup (1323.45 km^2), Baksa (1304.29 km^2), and Dhubri (1053.6 km^2). These calculations were performed using ArcGIS 10.8 with pixel-based area calculation methods.

Due to the Assam flood, many forested land and open trees were affected. Flood inundation and deforestation affect mainly south, northeast, west, and central parts of Assam. Figure 5a,b indicates the district-wise deforested land over Assam state. Figure 5b was overlapped map of deforested land in the NDVI map of Assam. Table 2 shows the district-wise affected areas are Kokrajhar (1942.36 km^2), Tinsukia (924.35 km^2), Dhemaji (1204.76 km^2), Dibrugarh (998.26 km^2), Lakhimpur (1590.34 km^2), Jorhat (875.34 km^2), Dimahasao (782.49 km^2), Cachar (1983.47 km^2), Karimganj (792.29 km^2), Karbi Anglong West (291.64 km^2), Nagaon (1103.17 km^2), Morigaon (893.54 km^2), Sonitpur (642.69 km^2), Kamrup (964.37 km^2), Baksa (673.17 km^2), and Dhubri (737.28 km^2).

Table 2. District-wise vegetation losses and flood inundation area of Assam flood, 2022.

Sl. No.	District Name	Total Area (km^2)	Affected Lands (km^2)		Affected Lands (%)	
			Vegetation Loss	Flood Inundation	Vegetation Loss	Flood Inundation
1	Kokraihar	3144.41	1942.36	2213.64	61.77	70.40
2	Tinsukia	3915.61	924.35	847.94	23.61	21.66
3	Dhemaji	2475.94	1204.76	1445.28	48.66	58.37
4	Dibrugarh	3435.57	998.26	698.78	29.06	20.34
5	Charaideo	1049.38	531.49	542.94	50.65	51.74
6	Sivasagar	1589.3	943.17	464.19	59.34	29.21
7	Lakhimpur	2904.82	1590.34	842.97	54.75	29.02
8	Majuli	1175.24	431.78	473.61	36.74	40.30
9	Jorhat	1941.79	875.34	942.91	45.08	48.56
10	Biswanath	1827.27	431.28	794.68	23.60	43.49
11	Golaghat	3304.63	291.38	920.98	8.82	27.87
12	Dimahasao	4909.73	782.49	1759.34	15.94	35.83

Table 2. *Cont.*

Sl. No.	District Name	Total Area (km^2)	Affected Lands (km^2)		Affected Lands (%)	
			Vegetation Loss	Flood Inundation	Vegetation Loss	Flood Inundation
13	Karbi Anglong	7242.34	324.16	552.96	4.48	7.64
14	Cachar	3781.94	1983.47	2253.29	52.45	59.58
15	Hailakandi	1362.14	539.79	831.38	39.63	61.03
16	Karimganj	1754.59	792.29	1095.16	45.16	62.42
17	Hojai	1500.14	439.26	991.64	29.28	66.10
18	Karbi Anglong West	3013.16	291.64	1795.28	9.68	59.58
19	Nagaon	2546.07	1103.17	1594.72	43.33	62.63
20	Morigaon	1587.23	893.54	1056.38	56.30	66.55
21	Kamrup Metropolitan	971.89	153.78	595.1	15.82	61.23
22	Sonitpur	3424.74	642.69	1549.24	18.77	45.24
23	Danrang	1464.17	831.29	1164.27	56.78	79.52
24	Udalguri	2070.24	539.73	1253.15	26.07	60.53
25	Kamrup	3087.22	964.37	1323.45	31.24	42.87
26	Nalbari	969.61	461.28	519.5	47.57	53.58
27	Goalpara	2001.53	356.57	478.36	17.81	23.90
28	Baksa	2531.87	673.17	1304.29	26.59	51.51
29	Barpeta	2261.41	429.79	531.18	19.01	23.49
30	Chirang	1972.81	619.81	1024.9	31.42	51.95
31	Bongaigaon	966.23	419	594.26	43.36	61.50
32	South Salmara-mankachar	682.5	364.19	393.12	53.36	57.60
33	Dhubri	1565.81	737.28	1053.6	47.09	67.29

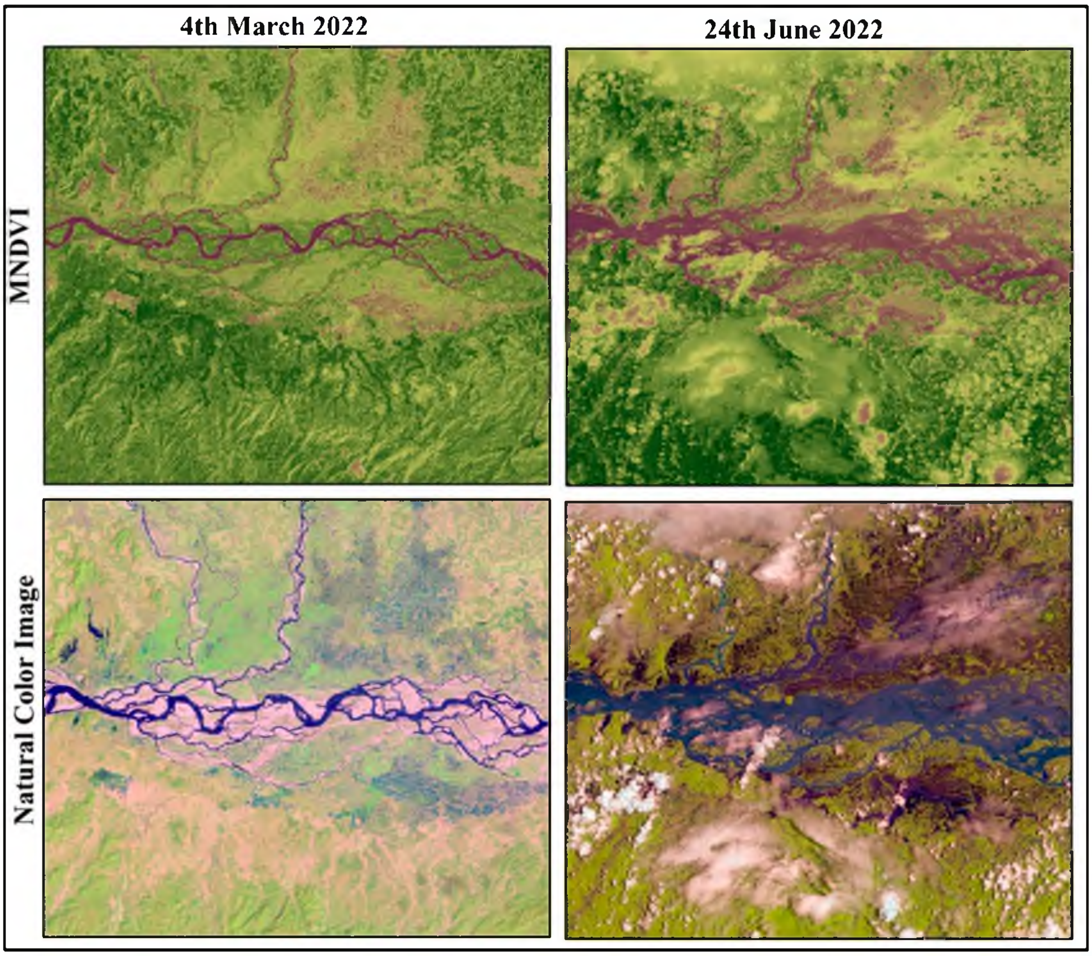

Figure 3. MNDWI and natural color image of Landsat 8 OLI/TIRS for space-based flooded area identification.

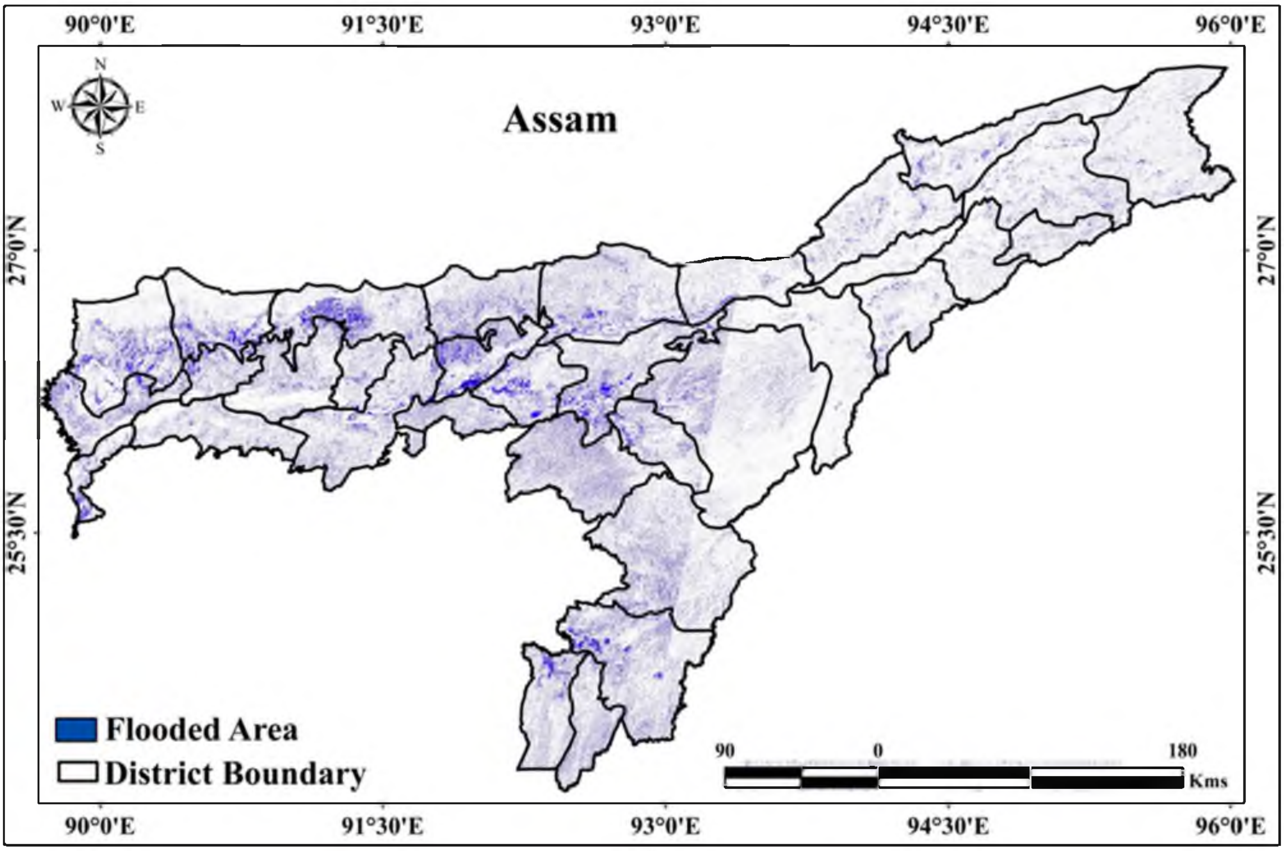

(a)

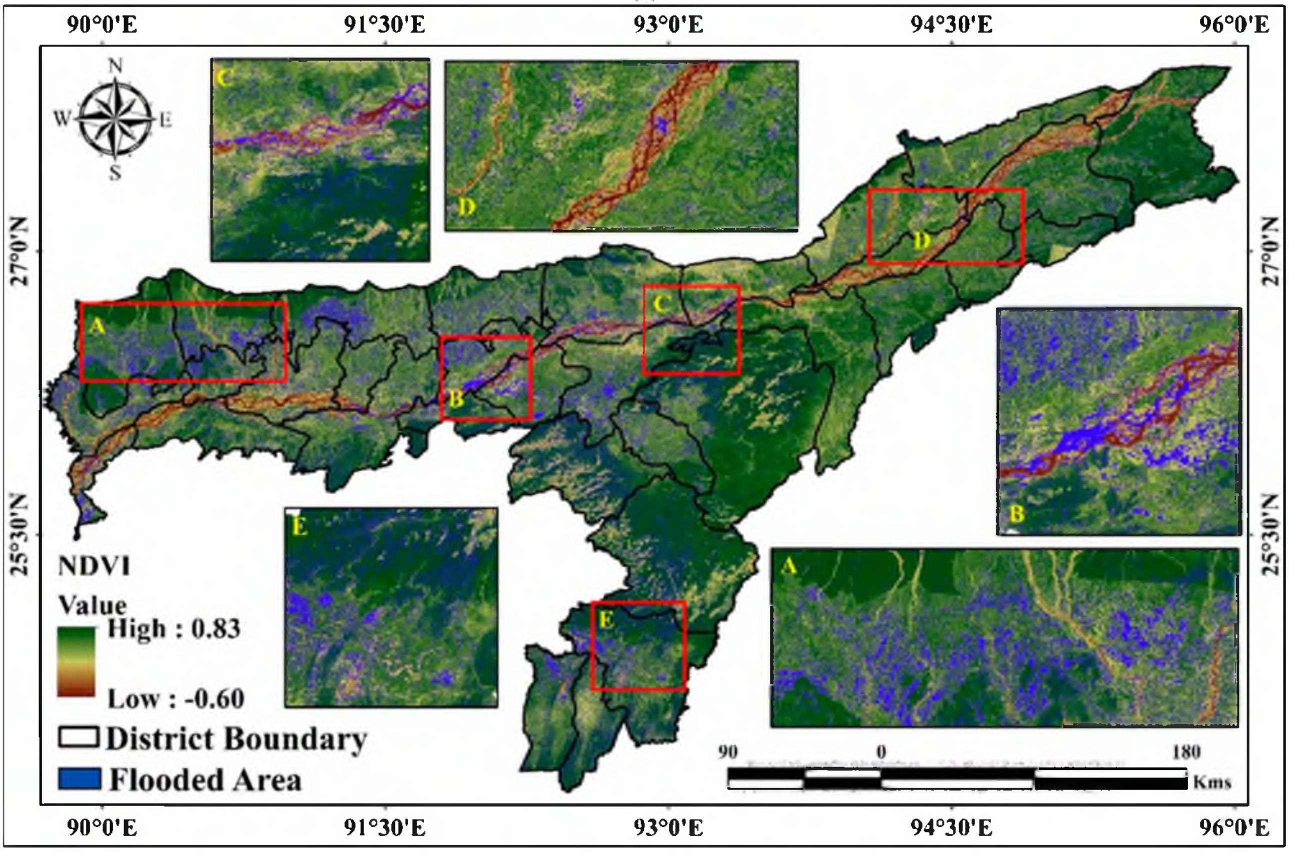

(b)

Figure 4. (**a**) Flooded area of Assam flood; (**b**) flood inundation area of Assam flood.

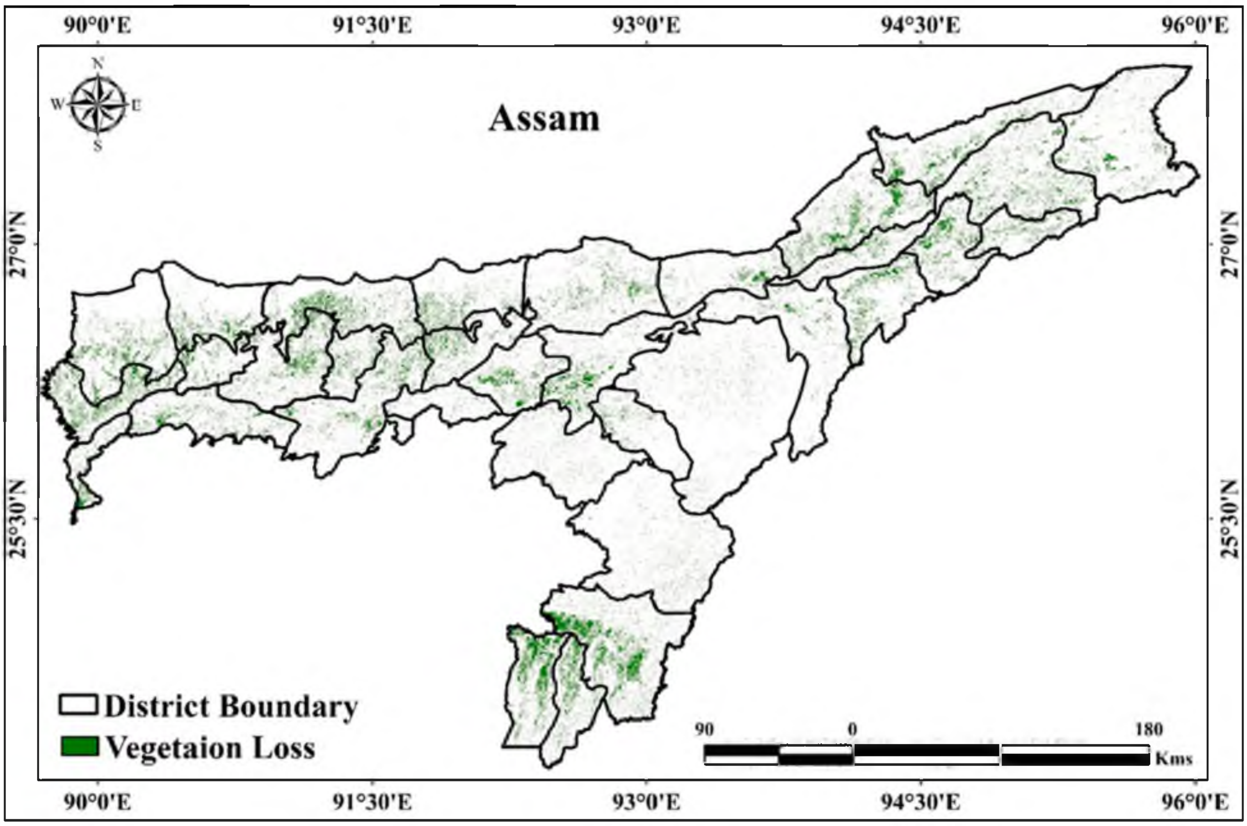

(a)

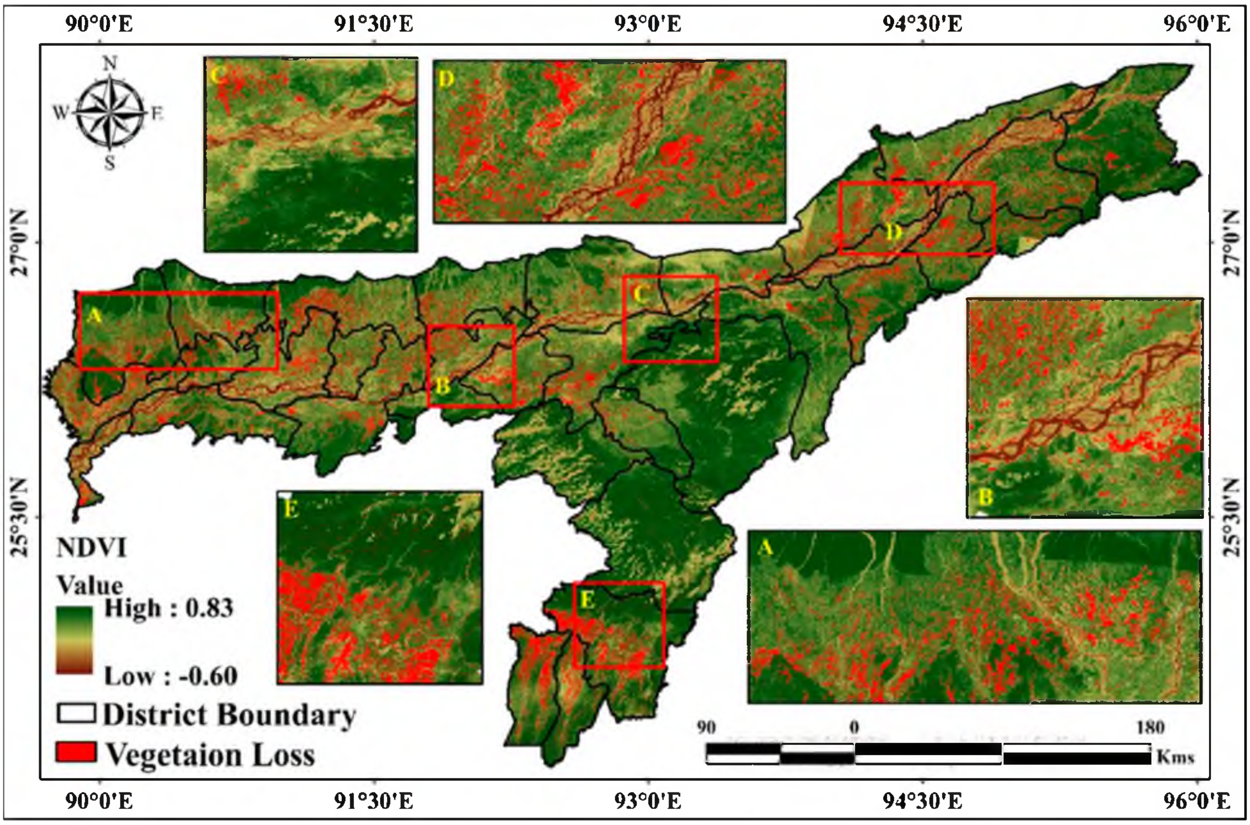

(b)

Figure 5. (**a**) Affected vegetation area of Assam flood; (**b**) affected vegetation area during Assam flood.

4.2. Affected LULC Areas

Identifying the areas of land affected by land use and land cover LULC change is a crucial aspect of flood investigations. Agricultural lands, trees, and settlements are particularly susceptible to flood damage. The flood inundation-related hazard has significantly impacted numerous cities and towns in Assam state. The overlap technique was employed to determine the extent of the affected LULC areas. Flood and deforested lands were calculated using the ArcGIS v10.8 platform. The distribution of affected lands (flood inundation and deforestation) across different districts is presented in Figure 6, while Figure 7 and Table 2 provide further details on the impacted LULC categories resulting from the Assam flood. Approximately 17,417.8 km^2 of croplands were affected by the flood, along with several other LULC classes (Table 3).

Table 3. Affected LULC classes during the Assam flood, 2022.

Sl. No.	District Name	Total Area (km^2)	Affected Land (km^2)					
			Trees	Waterbody	Bare Land	Crops Land	Built-Up Land	Flooded Vegetation
1	Kokraihar	3144.41	421.14	21.34	1.33	1637.25	120.24	12.34
2	Tinsukia	3915.61	142.31	42.85	2.68	539.53	99.53	21.04
3	Dhemaji	2475.94	631.24	29.54	0.95	644.16	124.28	15.11
4	Dibrugarh	3435.57	314.25	42.39	1.29	188.41	110.29	42.15
5	Charaideo	1049.38	349.29	32.14	2.64	79.39	59.34	20.14
6	Sivasagar	1589.3	195.49	15.26	10.59	114.48	83.16	45.21
7	Lakhimpur	2904.82	248.74	11.32	26.34	478.89	62.94	14.74
8	Majuli	1175.24	172.29	28.92	19.26	152.37	49.53	51.24
9	Jorhat	1941.79	249.42	13.24	24.62	516.55	123.59	15.49
10	Biswanath	1827.27	462.15	13.27	16.34	206.82	20.89	75.21
11	Golaghat	3304.63	624.83	20.21	31.21	127.58	92.46	24.69
12	Dimahasao	4909.73	1324.89	15.32	2.18	31.69	21.05	85.21
13	Karbi Anglong	7242.34	1954.76	8.25	4.32	29.12	19.23	15.42
14	Cachar	3781.94	1642.34	4.37	11.29	27.09	69.95	18.25
15	Hailakandi	1362.14	231.42	12.37	16.32	513.18	15.9	42.19
16	Karimganj	1754.59	314.52	11.12	19.23	664.1	42.95	43.24
17	Hojai	1500.14	214.59	11.58	14.52	691.97	29.56	29.42
18	Karbi Anglong West	3013.16	954.23	14.37	14.32	721.48	19.53	71.35
19	Nagaon	2546.07	521.16	21.29	16.37	964.34	52.31	19.25
20	Morigaon	1587.23	312.19	22.34	8.21	641.92	29.59	42.13
21	Kamrup Metropolitan	971.89	103.29	22.95	9.12	277.91	120.59	61.24
22	Sonitpur	3424.74	109.42	16.23	4.37	1351.89	42.38	24.95
23	Danrang	1464.17	204.46	10.21	2.59	881.63	53.24	12.14
24	Udalguri	2070.24	207.53	21.36	3.61	955.72	23.28	41.65
25	Kamrup	3087.22	546.32	31.42	1.25	614.72	95.56	34.18
26	Nalbari	969.61	246.1	12.34	2.34	145.13	82.35	31.24
27	Goalpara	2001.53	431.25	11.26	5.24	1460.33	55.93	37.52
28	Baksa	2531.87	304.86	16.52	9.62	884.18	49.57	39.54
29	Barpeta	2261.41	346.59	13.29	4.37	55	82.42	29.51
30	Chirang	1972.81	249.53	14.32	2.53	623.16	92.15	43.21
31	Bongaigaon	966.23	164.95	19.73	2.52	335.31	49.54	22.21
32	South Salmara-mankachar	682.5	82.43	18.39	3.26	193.45	82.34	13.25
33	Dhubri	1565.81	201.79	21.35	1.28	723.05	92.16	13.97

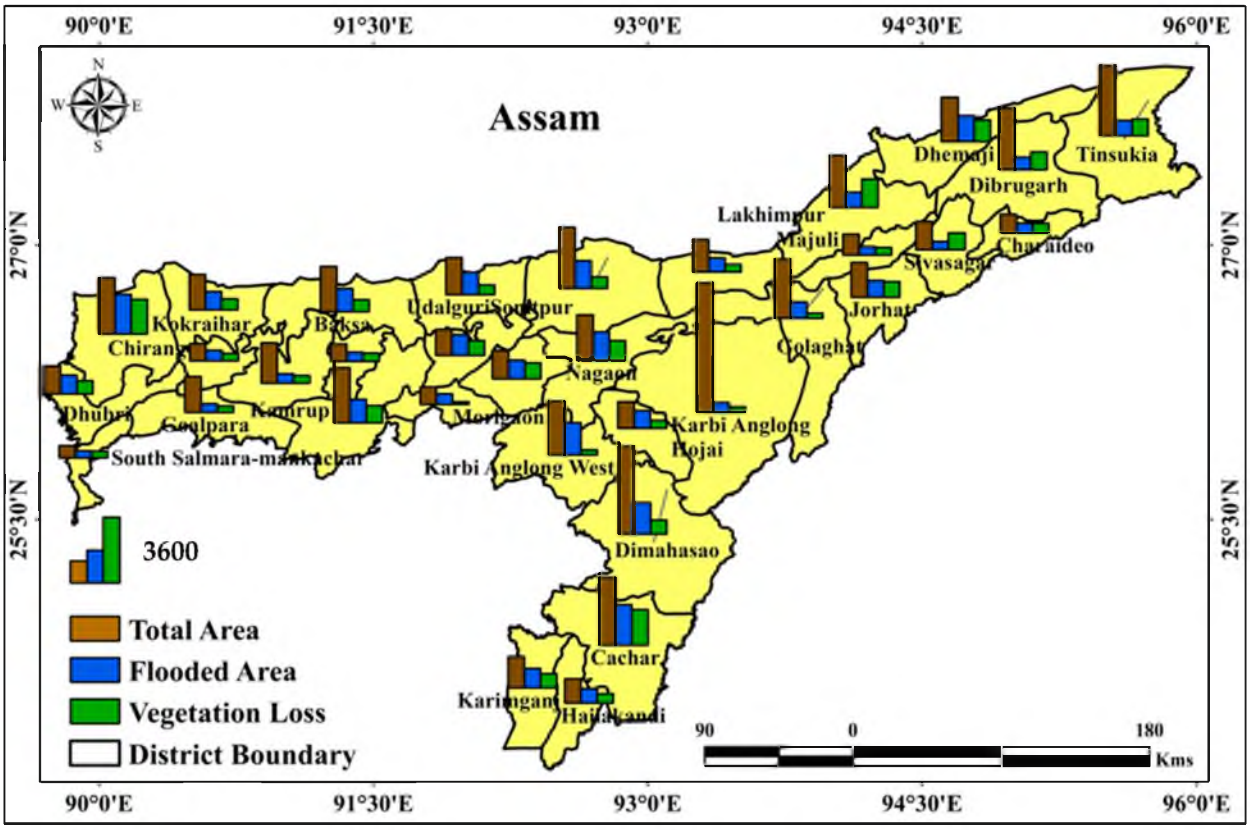

Figure 6. Affected land of Assam flood during 2022.

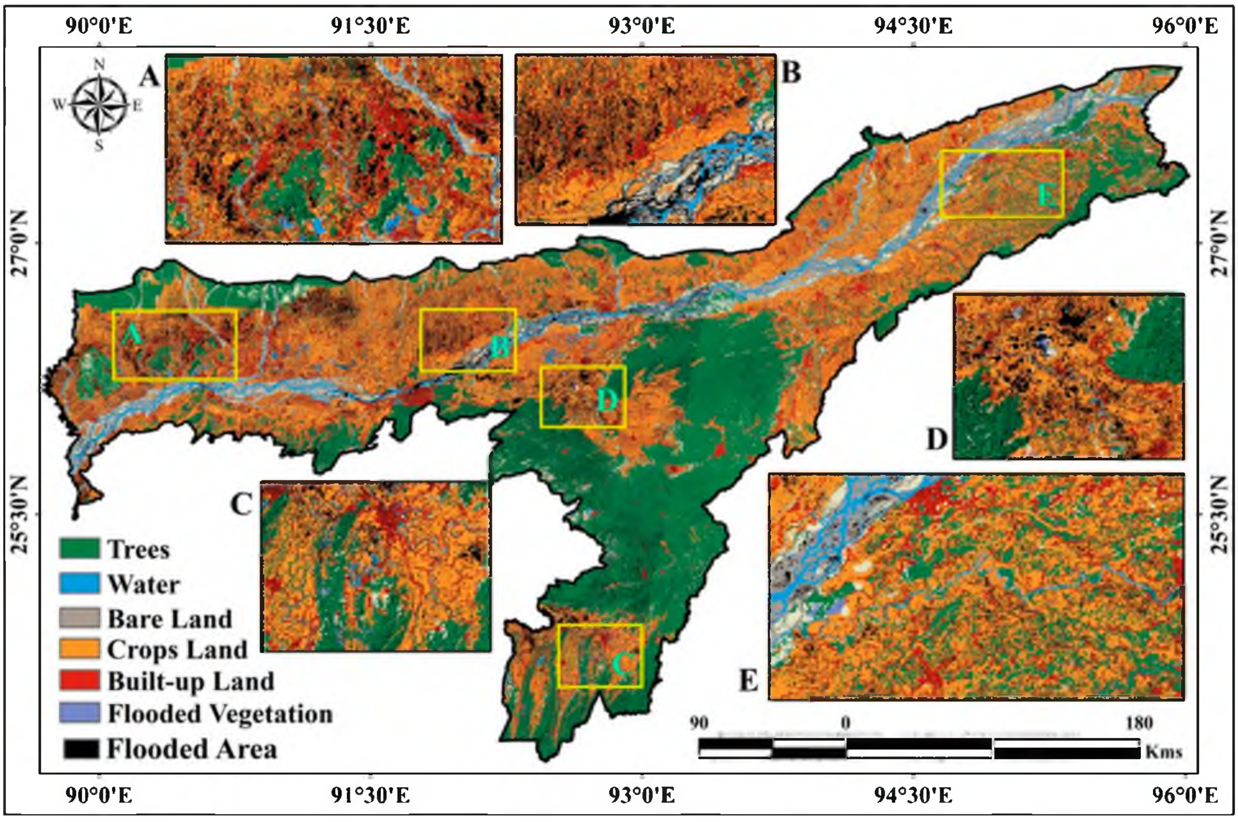

Figure 7. Affected land use and land cover classes of Assam flood during 2022.

The areas most affected by the flood in terms of built-up lands include Kamrup Metropolitan (120.59 km^2), Kokrajhar (120.24 km^2), Dhemaji (124.28 km^2), Dibrugarh (110.29 km^2), Jorhat (123.59 km^2), and Dhubri (92.16 km^2). The districts with the highest impact on croplands are Kokrajhar (1637.25 km^2), Dhemaji (644.16 km^2), Jorhat (516.55 km^2), Hailakandi (513.18 km^2), Karimganj (664.1 km^2), Hojai (691.97 km^2), Karbi Anglong West (721.48 km^2), Nagaon (964.34 km^2), Sonitpur (1351.89 km^2), Danrang (881.63 km^2), and Baksa (884.18 km^2). The analysis of flood inundation and deforested land indicates a large affected area due to the 2022 flood, which caused significant economic and human losses. Proper planning, management, and adaptation strategies are needed to protect the environment. The findings of this study can also assist in future disaster management planning and the development of new adaptation strategies. Dhemaji, Jorhat, Hailakandi, Karimganj, and Sonitpur are the most severely affected areas. The flood has had detrimental effects on vegetation, cropland, flood inundation, and soil moisture levels, resulting in substantial economic losses. Therefore, it is crucial to implement sustainable planning for flood hazard management to reduce risks and improve future disaster management efforts. Various techniques, such as stone or concrete riprap, vegetation plantation, and sediment transportation, can mitigate flood effects and reduce inundation in riverine areas. Innovative approaches and adaptation planning may also prove beneficial in mitigating the impacts of flood inundation in the study area.

5. Discussion

Assam's flood problem is arguably the most severe and unique because it differs significantly from that of other states in terms of the magnitude and duration of floods as well as the volume of erosion. According to the Water Resources Department, Govt. of Assam, the entire flood-affected area of the country is around 10.2% of the overall parts of the country. In contrast, the flood-affected areas of Assam are 39.58% of the entire parts of the state (https://waterresources.assam.gov.in/, accessed on 22 August 2022). In 2022, flashfloods of great magnitude occurred because of cloud bursts in catchment zones of Upper Assam. Flood inundation mapping and monitoring of the affected lands are more important for future planning and management purpose. Assam is mainly a flood susceptible state. Future, the predictable intensification of the rainfall, its strength, and enhanced summer flows might lead to additional frequent incidences of flood and flash floods in Assam's Brahmaputra River valley [48]. In highly flood-prone regions, people have lesser poverty incidence and higher spending [49]. Continuous SAR datasets were developed throughout the flood because of the lengthier wavelength and its sensitivity near the target's geometrical, dielectric, and structural possessions. Flood inundation diagrams have been produced by dual-polarized Sentinel-1 SAR datasets [50]. The conceivable clarification might be fewer agriculturalists, additional administration relief, and better tribes with elevated substance in the high flood-prone regions. From the previous conversation, researchers find that flooding increases people's susceptibility to poverty. In contrast, poor people and those in highly flood-prone regions were more susceptible to floods [48]. Assam is gradually affected by several flood disaster-related phenomena, where life losses, economic losses, deforestation, and environmental degradation are noticed. Vegetation areas are more important for the environment, but anthropogenic activities and natural phenomena gradually decrease vegetation. Therefore, environmental protection is the main concerning factor currently. Three datasets were applied to this analysis: Landsat 8 OLI/TIRS, Sentinel 1 GRD, and Sentinel 2 MSI datasets. Landsat has a 30 m resolution, which has heterogeneity-related problems. Sentinel 2 data is multispectral and needs cloud-free data for analysis. Ground-based analysis affected the overall accuracy of the outcomes, but this study's results are mostly applied satellite datasets due to the need for more information. Some future studies may help in the forecasting of the disaster, like year-wise flood inundation and deforestation measurement, canopy height, biomass estimation, decadal shoreline change, sediment transportation, and simulation of the shoreline is more helpful for awareness purposes for future disaster management teams and local administrative bodies for sustainable forest restoration.

6. Conclusions

Assam state experiences annual flooding, resulting in significant economic and life losses. In 2022, multiple flood events occurred. Effective planning, management, awareness, adaptation strategies, and administrative development are crucial in preventing flood inundation and related environmental degradation. This investigation focused on identifying Assam's 2022 flood inundation and associated deforestation. Flood inundation mapping was performed using C-band Sentinel-1 SAR data, while space-based flood inundation mapping using MNDWI was carried out using Landsat 8 OLI/TIRS datasets. The results revealed that Kokrajhar, Cachar, Nagaon, Dimahasao, and Karbi Anglong West were the most flood-inundated areas, covering approximately 2213.68 km^2, 2253.29 km^2, 1594.72 km^2, 1759.34 km^2, and 1795.28 km^2, respectively. Vegetated lands were also affected, particularly in Kokrajhar (1942.36 km^2), Lakhimpur (1590.34 km^2), Cachar (1983.47 km^2), and Nagaon (1103.17 km^2) districts.

This research's scientific contribution lies in identifying flood inundation and assessing vegetation damage caused by the 2022 Assam flood. This is crucial for understanding hazard vulnerability using Sentinel-1 SAR datasets and the GEE platform. The study reveals that the Brahmaputra River area of Assam is highly affected by floods, with a significant impact on forested areas. This study fills the gap in knowledge regarding the recent 2022 flood and is essential for hazard vulnerability assessment. The flood has led to food shortages, loss of life, economic losses, and other problems, including damage to railway stations and lines. Soil erosion and deforestation resulting from flood inundation have also affected animals (0.9 million) and humans (1.9 million affected and 54 lives lost). The use of Sentinel-1 SAR datasets allowed for the calculation of flood inundation and deforested areas in the 2022 Assam flood. However, it is important to acknowledge limitations, such as the need for field validation and the inability of satellite-based investigations to capture the full extent of the results. The actual number of affected people may be higher than the recorded figures.

Future studies should focus on identifying flood inundation-related issues in Assam, including analyzing the Brahmaputra River's flow, investigating sediment deposition, studying soil erosion and landslides, assessing human-induced deforestation, and examining flood-prone areas. The findings of this study are valuable for disaster management departments and policymaking.

Author Contributions: Conceptualization, B.H., J.B., F.T., S.S., B.A.-R. and Z.M.Y.; Data curation, B.H.; Formal analysis, B.H., S.B., P.B., P.D., C.B.P., B.A.-R. and Z.M.Y.; Investigation, B.H., S.B., P.B., P.D., J.B., C.B.P., B.A.-R. and Z.M.Y.; Methodology, B.H., S.B. and P.B.; Project administration, F.T. and Z.M.Y.; Resources, P.D., J.B., B.A.-R. and Z.M.Y.; Software, B.H. and P.B.; Supervision, S.S. and Z.M.Y.; Validation, B.H., S.B., P.D., J.B., F.T., S.S., C.B.P., B.A.-R. and Z.M.Y.; Visualization, P.B., F.T., S.S., C.B.P., B.A.-R. and Z.M.Y.; Writing—original draft, B.H., S.B., P.B., P.D., J.B., F.T., S.S., C.B.P., B.A.-R. and Z.M.Y.; Writing—review and editing, B.H., J.B., F.T., S.S., C.B.P., B.A.-R. and Z.M.Y. All authors have read and agreed to the published version of the manuscript.

Funding: This research received no external funding.

Institutional Review Board Statement: Not applicable.

Informed Consent Statement: Not applicable.

Data Availability Statement: Data can be provided upon request.

Acknowledgments: Z.M.Y. and B.A.-R. would like to acknowledge the support received by the KFUPM, Saudi Arabia.

Conflicts of Interest: The authors declare no conflict of interest.

References

1. Zarei, M.; Bozorg-Haddad, O.; Baghban, S.; Delpasand, M.; Goharian, E.; Loáiciga, H.A. Machine-Learning Algorithms for Forecast-Informed Reservoir Operation (FIRO) to Reduce Flood Damages. *Sci. Rep.* **2021**, *11*, 24295. [CrossRef]
2. Brakenridge, G.R. Flood Risk Mapping from Orbital Remote Sensing. In *Global Flood Hazard*; John Wiley & Sons: Hoboken, NJ, USA, 2018; pp. 43–54.
3. Sanyal, J.; Lu, X.X. GIS-based Flood Hazard Mapping at Different Administrative Scales: A Case Study in Gangetic West Bengal, India. *Singap. J. Trop. Geogr.* **2006**, *27*, 207–220. [CrossRef]
4. Danandeh Mehr, A.; Akdegirmen, O. Estimation of Urban Imperviousness and Its Impacts on Flashfloods in Gazipaşa, Turkey. *Knowl. Based Eng. Sci.* **2021**, *2*, 9–17. [CrossRef]
5. Starkel, L. The Role of Catastrophic Rainfall in the Shaping of the Relief of the Lower Himalaya (Darjeeling Hills). *Geogr. Pol.* **1972**, *21*, 103–147.
6. Gupta, A. *Large Floods as Geomorphic Events in the Humid Tropics*; Wiley: Hoboken, NJ, USA, 1988.
7. Wolman, M.G.; Gerson, R. Relative Scales of Time and Effectiveness of Climate in Watershed Geomorphology. *Earth Surf. Process.* **1978**, *3*, 189–208. [CrossRef]
8. Rahman, M.R.; Thakur, P.K. Detecting, Mapping and Analysing of Flood Water Propagation Using Synthetic Aperture Radar (SAR) Satellite Data and GIS: A Case Study from the Kendrapara District of Orissa State of India. *Egypt. J. Remote Sens. Space Sci.* **2018**, *21*, S37–S41. [CrossRef]
9. Ghosh, S.; Kumar, R.; Pandey, U.; Srivastava, P.; Mehra, S. Recent Flood Event in Kaziranga National Park, Assam, India as Assessed Using Remote Sensing Data. *Curr. Sci.* **2018**, *115*, 821. [CrossRef]
10. Pal, I.; Singh, S.; Walia, A. Flood Management in Assam, INDIA: A Review of Brahmaputra Floods, 2012. *Int. J. Sci. Res. Publ.* **2013**, *3*, 1.
11. Bandyopadhyay, J.; Rahaman, S.K.H.; Karan, C. Agricultural Potential Zone Mapping with Surface Water Resource Management Using Geospatial Tools for Jhargram District, West Bengal, India. *Knowl. Based Eng. Sci.* **2023**, *4*, 1–18.
12. Doocy, S.; Daniels, A.; Murray, S.; Kirsch, T.D. The Human Impact of Floods: A Historical Review of Events 1980-2009 and Systematic Literature Review. *PLoS Curr.* **2013**, *5*. [CrossRef]
13. Wahlstrom, M.; Guha-Sapir, D. *The Human Cost of Weather-Related Disasters 1995–2015*; UNISDR: Geneva, Switzerland, 2015.
14. Water Resources of Bangladesh. 2009. Available online: https://washdata.org/sites/default/files/documents/reports/2019-06/Bangladesh-2009-MICS-water-quality-report.pdf (accessed on 22 August 2022).
15. Kale, V.S. Geomorphic Effects of Monsoon Floods on Indian Rivers. In *Flood Problem and Management in South Asia*; Springer: Berlin/Heidelberg, Germany, 2003; pp. 65–84.
16. Venkatachary, K.V.; Bandyopadhyay, K.; Bhanumurthy, V.; Rao, G.S.; Sudhakar, S.; Pal, D.K.; Das, R.K.; Sarma, U.; Manikiam, B.; Rani, H.C.M. Defining a Space-Based Disaster Management System for Floods: A Case Study for Damage Assessment Due to 1998 Brahmaputra Floods. *Curr. Sci.* **2001**, *80*, 369–377.
17. Sharma, V.K.; Mishra, N.; Shukla, A.K.; Yadav, A.; Rao, G.S.; Bhanumurthy, V. Satellite Data Planning for Flood Mapping Activities Based on High Rainfall Events Generated Using TRMM, GEFS and Disaster News. *Ann. GIS* **2017**, *23*, 131–140. [CrossRef]
18. Devrani, R.; Srivastava, P.; Kumar, R.; Kasana, P. Characterization and Assessment of Flood Inundated Areas of Lower Brahmaputra River Basin Using Multitemporal Synthetic Aperture Radar Data: A Case Study from NE India. *Geol. J.* **2022**, *57*, 622–646. [CrossRef]
19. Dhar, O.N.; Nandargi, S. A Study of Floods in the Brahmaputra Basin in India. *Int. J. Climatol. A J. R. Meteorol. Soc.* **2000**, *20*, 771–781. [CrossRef]
20. Bhardwaj, P.; Singh, O. Climatological Characteristics of Bay of Bengal Tropical Cyclones: 1972–2017. *Theor. Appl. Climatol.* **2019**, *139*, 615–629. [CrossRef]
21. Kadavi, P.; Lee, C.-W.; Lee, S. Application of Ensemble-Based Machine Learning Models to Landslide Susceptibility Mapping. *Remote Sens.* **2018**, *10*, 1252. [CrossRef]
22. Bhattachaiyya, N.N.; Bora, A.K. Floods of the Brahmaputra River in India. *Water Int.* **1997**, *22*, 222–229. [CrossRef]
23. Debbarma, A.; Deen, S. Flood Disaster Management in Assam. *Shodh Sanchar Bull.* **2020**, *19*, 10.
24. Sarma, J.N.; Acharjee, S. A GIS Based Study on Bank Erosion by the River Brahmaputra around Kaziranga National Park, Assam, India. *Earth Syst. Dynam. Discuss.* **2012**, *3*, 1085–1106.
25. Borah, S.B.; Sivasankar, T.; Ramya, M.N.S.; Raju, P.L.N. Flood Inundation Mapping and Monitoring in Kaziranga National Park, Assam Using Sentinel-1 SAR Data. *Environ. Monit. Assess.* **2018**, *190*, 1–11. [CrossRef] [PubMed]
26. Grimaldi, S.; Xu, J.; Li, Y.; Pauwels, V.R.N.; Walker, J.P. Flood Mapping under Vegetation Using Single SAR Acquisitions. *Remote Sens. Environ.* **2020**, *237*, 111582. [CrossRef]
27. Townsend, P.A.; Foster, J.R. Assessing Flooding and Vegetation Structure in Forested Wetlands Using Radarsat SAR Imagery. *IEEE Int. Geosci. Remote Sens. Symp.* **2002**, *2*, 1171–1173.
28. Dong, J.; Xiao, X.; Menarguez, M.A.; Zhang, G.; Qin, Y.; Thau, D.; Biradar, C.; Moore, B., 3rd. Mapping Paddy Rice Planting Area in Northeastern Asia with Landsat 8 Images, Phenology-Based Algorithm and Google Earth Engine. *Remote Sens. Environ.* **2016**, *185*, 142–154. [CrossRef] [PubMed]

29. Dadhich, G.; Miyazaki, H.; Babel, M. Applications of Sentinel-1 Synthetic Aperture Radar Imagery for Floods Damage Assessment: A Case Study of Nakhon Si Thammarat, Thailand. *Int. Arch. Photogramm. Remote Sens. Spat. Inf. Sci.* **2019**, *XLII-2/W13*, 1927–1931. [CrossRef]
30. Amitrano, D.; Di Martino, G.; Iodice, A.; Riccio, D.; Ruello, G. Unsupervised Rapid Flood Mapping Using Sentinel-1 GRD SAR Images. *IEEE Trans. Geosci. Remote Sens.* **2018**, *56*, 3290–3299. [CrossRef]
31. Surabuddin Mondal, M.; Sharma, N.; Kappas, M.; Garg, P.K. Modeling of Spatio-Temporal Dynamics of Land Use and Land Cover in a Part of Brahmaputra River Basin Using Geoinformatic Techniques. *Geocarto Int.* **2013**, *28*, 632–656. [CrossRef]
32. Assam Flood Report. 2022. Available online: https://ndrf.gov.in/operations/assam-floods-2022 (accessed on 23 August 2022).
33. Goswami, D.C. Flood Forecasting in the Brahmaputra River, India: A Case Study. In *Regional Cooperation for Flood Disaster Mitigation in the Hindukush-Himalaya, ICIMOD Internal Report*; ICIMOD: Patan, Nepal, 2001.
34. Das, S.; Aggarwal, M. Why Assam Faces Floods Every Year. 2017. Available online: https://www.livemint.com/Politics/JEGERRSFHOVCAm86Pd1tnL/Why-Assam-faces-floods-every-year.html (accessed on 22 May 2023).
35. Assam State Disaster Management Authority. 2016. Available online: https://reliefweb.int/report/india/government-assam-assam-state-disaster-management-authority-flood-report-26-apr-2016 (accessed on 23 August 2022).
36. Halder, B.; Ahmadianfar, I.; Heddam, S.; Mussa, Z.H.; Goliatt, L.; Tan, M.L.; Sa'adi, Z.; Al-Khafaji, Z.; Al-Ansari, N.; Jawad, A.H. Machine Learning-Based Country-Level Annual Air Pollutants Exploration Using Sentinel-5P and Google Earth Engine. *Sci. Rep.* **2023**, *13*, 7968. [CrossRef]
37. Ghute, B.B.; Shaikh, M.B.; Halder, B. Impact Assessment of Natural and Anthropogenic Activities Using Remote Sensing and GIS Techniques in the Upper Purna River Basin, Maharashtra, India. *Model. Earth Syst. Environ.* **2023**, *9*, 1507–1522. [CrossRef]
38. Chung, H.-W.; Liu, C.-C.; Cheng, I.-F.; Lee, Y.-R.; Shieh, M.-C. Rapid Response to a Typhoon-Induced Flood with an SAR-Derived Map of Inundated Areas: Case Study and Validation. *Remote Sens.* **2015**, *7*, 11954–11973. [CrossRef]
39. Zhang, B.; Wdowinski, S.; Oliver-Cabrera, T.; Koirala, R.; Jo, M.J.; Osmanoglu, B. Mapping the Extent and Magnitude of Sever Flooding Induced by Hurricane Irma with Multi-Temporal Sentinel-1 Sar and Insar Observations. *Int. Arch. Photogramm. Remote Sens. Spat. Inf. Sci.* **2018**, *XLII–3*, 2237–2244. [CrossRef]
40. Sibtain, M.; Li, X.; Saleem, S. A Multivariate and Multistage Medium- and Long-Term Streamflow Prediction Based on an Ensemble of Signal Decomposition Techniques with a Deep Learning Network. *Adv. Meteorol.* **2020**, *2020*, 8828664. [CrossRef]
41. Lu, J.; Giustarini, L.; Xiong, B.; Zhao, L.; Jiang, Y.; Kuang, G. Automated Flood Detection with Improved Robustness and Efficiency Using Multi-Temporal SAR Data. *Remote Sens. Lett.* **2014**, *5*, 240–248. [CrossRef]
42. McFEETERS, S.K.; Gorelick, N.; Hancher, M.; Dixon, M.; Ilyushchenko, S.; Thau, D.; Moore, R.; Hassan, M.M.; Ash, K.; Abedin, J.; et al. Integration of Remote Sensing Data and GIS for Accurate Mapping of Flooded Areas. *Remote Sens.* **2018**, *11*, 990–1002. [CrossRef]
43. Tamiminia, H.; Salehi, B.; Mahdianpari, M.; Quackenbush, L.; Adeli, S.; Brisco, B. Google Earth Engine for Geo-Big Data Applications: A Meta-Analysis and Systematic Review. *ISPRS J. Photogramm. Remote Sens.* **2020**, *164*, 152–170. [CrossRef]
44. Xu, H. Modification of Normalized Difference Water Index (NDWI) to Enhance Open Water Features in Remotely Sensed Imagery. *Int. J. Remote Sens.* **2006**, *27*, 3025–3033. [CrossRef]
45. Halder, B.; Bandyopadhyay, J.; Banik, P. Evaluation of the Climate Change Impact on Urban Heat Island Based on Land Surface Temperature and Geospatial Indicators. *Int. J. Environ. Res.* **2021**, *15*, 819–835. [CrossRef]
46. Coleman, J.M. Brahmaputra River: Channel Processes and Sedimentation. *Sediment. Geol.* **1969**, *3*, 129–239. [CrossRef]
47. Bristow, C.S.; Smith, N.; Rogers, J. Gradual Avulsion, River Metamorphosis and Reworking by Underfit Streams: A Modern Example from the Brahmaputra River in Bangladesh and a Possible Ancient Example in the Spanish Pyrenees. *Fluv. Sedimentol. VI* **1999**, *28*, 221–230.
48. Mahanta, R.; Das, D. Flood induced vulnerability to poverty: Evidence from Brahmaputra Valley, Assam, India. *Int. J. Disaster Risk Reduct.* **2017**, *24*, 451–461. [CrossRef]
49. Mandal, R.; Bezbaruah, M.P. Diversification of cropping pattern: Its determinants and role in flood affected agriculture of Assam Plains. *Indian J. Agric. Econ.* **2013**, *68*, 169–181.
50. Mandal, R. Flood, cropping pattern choice and returns in agriculture: A study of Assam plains, India. *Econ. Anal. Policy* **2014**, *44*, 333–344. [CrossRef]